

## Compositions, Structures, and Thermal Behavior of Nickel-Containing Minerals in the Lizardite-Nepouite Series

G. W. BRINDLEY AND HSIEN-MING WAN

*Department of Geosciences, and Materials Research Laboratory  
The Pennsylvania State University, University Park, Pennsylvania 16802*

### Abstract

Fourteen samples of nickel-containing serpentine minerals, all of which resemble lizardite, have been studied by X-ray powder diffraction, thermogravimetric and chemical analysis, and electron microscopy. Those containing more than 1.5 Ni ions per formula unit  $R_3Si_2O_5(OH)_4$  are called nepouites, and those with fewer Ni ions are called nickel lizardites. The samples vary considerably in structural order and the nepouites generally are less well-ordered than the nickel lizardites. Among the latter, two show clear evidence for a 2-layer orthogonal structure, and the diffracted intensities correspond generally with the *2Or* polymorph described by Bailey. Thermogravimetric analysis of these minerals shows that hydroxyl ions are retained after the first stage of reaction when the 7.2 Å basal spacing is lost and a long spacing, LS-phase appears with a spacing in the range 14-11 Å. It is suggested that this phase is similar to a chlorite after the first stage of dehydroxylation. All the samples studied show, to varying extents, the formation of an LS-phase. Nepouites also show a second transitional phase, which is face-centered cubic, and appears to be a finely divided form of nickel oxide. The high-temperature phases are olivine and enstatite from low-nickel materials, and olivine and cristobalite from high-nickel materials.

### Introduction

Nickel-containing minerals in the serpentine group resemble mainly lizardite and chrysotile. A nickel analog of chrysotile has been named pecoraite (Faust, *et al.*, 1969) and the name nepouite, introduced by Glasser (1907), has been redefined by Maksimovic (1973) for a nickel analog of lizardite. A nickel analog of antigorite, used in the strict sense of a mineral with a long superlattice *a* parameter, has not been observed. A nickel analog of the six-layer orthoserpentine (Brindley and von Knorring, 1954; Zussman and Brindley, 1957) has been synthesized by Jasmund and Sylla (1971a, b).

In a recent survey of garnierites (Brindley and Pham Thi Hang, 1973), where this term was used in a general sense, only four samples of serpentine-type minerals were obtained sufficiently pure for chemical analysis, and only two additional samples merited thermal study. In a continuation of this work, the number of serpentine-type samples has been increased to fourteen. They are all predominantly of the lizardite-nepouite type. The compositions range from low to high contents of NiO, and there are con-

siderable variations in the degree of structural order, and in the thermal transformations.

### Experimental Procedures

More than sixty mineral samples from many localities donated by industrial companies, museums, and individuals, and a few collected by ourselves, have been surveyed in order to obtain material suitable for the present work. The prominent green color of nickel-containing silicates enables them to be hand-picked under a binocular microscope, but subsequent X-ray diffraction analysis shows that many are mixtures. Material for detailed study was selected on the basis of (1) a basal spacing of about 7.2 Å and other X-ray data broadly consistent with serpentine-type structures, and (2) freedom from X-ray observable impurities. A Philips Norelco diffractometer was used with filtered  $CuK\alpha$  radiation, a scanning rate of  $1^\circ (2\theta)/\text{min}$  and a recording rate of  $1 \text{ inch}/2^\circ (2\theta)$ . Purification of samples by flotation or chemical methods was avoided because of possible alteration of these very-fine grained materials.

Thermogravimetric measurements were combined with X-ray and thermal transformation studies by

heating duplicate samples of about 50-100 mg in small platinum containers in a step-wise manner from 110° to 1150°C. One sample of each pair was used for weight measurements and the other for X-ray examination. The samples were brought to constant weight at 110°C and then heated for periods of about 4 hours at temperature intervals of about 50-70°C. The samples were cooled in a desiccator prior to each set of measurements. After the final heating at around 1150°C, sufficient material was available for chemical analysis by atomic absorption methods using the technique of Medlin, Suhr, and Bodkin (1969) which utilizes lithium metaborate fusions in graphite crucibles. In most samples the proportion of iron was small, and was determined as Fe<sub>2</sub>O<sub>3</sub>. The amounts of material were too small to permit separate determinations of ferrous iron.

The following list gives the localities, donors, and original classification numbers of the samples studied:

- #1 Kwanson, Taitung, Taiwan (#3, K.S. Tung, I.T.R.I., Taipei)
- #2 Kwanson, Taitung, Taiwan (#1, K.S. Tung, I.T.R.I., Taipei)
- #3 Webster, North Carolina (#74-101, D.L.Bish)
- #4 Loma Pagnerra, Dominica (#108001, U.S. National Museum)
- #5 Valojoro, Madagascar (#112 857, Mus. Hist. Nat., Paris; S. Caillère)
- #6 Pomalaa, Indonesia (#S71-2b, International Nickel Co., Canada)
- #7 Morro do Niquel, Minas Gerais, Brazil (#MN6, G.W. Brindley)
- #8 Morro do Corisco, Liberdade, Brazil (#3996, P.de Souza Santos)
- #9 Riddle, Oregon (#HMC5, Hanna Mining Company)
- #10 New Caledonia (National Mus., Madrid; J.L. Martin Vivaldi)
- #11 Pavlos, Béotie, Greece (P. Robert, University of Paris)
- #12 Nakety, New Caledonia (#122793, U.S. National Museum)
- #13 New Caledonia (#R4697, U.S. National Museum)
- #14 New Caledonia (Donor and origin uncertain)

In the present text, we shall refer to all samples by the numbers 1-14 preceding each description.

#### Chemical Analyses and Structural Formulae

Table 1 records the chemical analyses of the fourteen selected materials, and their structural formulae

evaluated on the basis of (a) a total cation valence of 14, and (b) a total of 3.00 equivalent octahedral cations, taken as  $\Sigma R^{2+} + \frac{2}{3} R^{3+}$ . The proportions of Na<sup>+</sup>, K<sup>+</sup> and Ca<sup>2+</sup> are small in all samples and are omitted from the formulae in Table 1 (b).

The minerals are labelled lizardites or nickel lizardites when the number of nickel ions in the formula derived by method (a) is less than 1.5, and nepouites when the number is greater than 1.5. The division corresponds to about 30 wt percent NiO. The term nickel lizardite is used when NiO exceeds 0.5 wt percent, which is an arbitrary division.

In lizardite samples 1 and 2 (Table 1), the Si ions fill respectively 1.93 and 1.95 of the tetrahedral positions and Al ions are added to bring the total to 2.00. The equivalent octahedral cations are respectively 3.03 and 3.02, and the H<sub>2</sub>O + values are 2.25 and 2.04 in place of the ideal 2H<sub>2</sub>O which corresponds to the formula R<sub>3</sub>Si<sub>2</sub>O<sub>6</sub>(OH)<sub>4</sub>. It makes no significant difference for these two samples whether the formulae are derived by method (a) or by method (b).

The nickel lizardites and nepouites treated by method (a) depart considerably from the ideal formula. Thus for samples 3 to 14, the average numbers of cations and water molecules are as follows: Si ions, 2.15 ± 0.04, equivalent octahedral cations, 2.69 ± 0.08, and H<sub>2</sub>O molecules, 2.06 ± 0.14. The excess of Si ions and the deficiency of equivalent octahedral cations are related arithmetically by the requirement that the total cation valence is +14. The excess of Si over 2.00 must equal one-half the deficiency of octahedral cations below 3.00. The H<sub>2</sub>O + content fluctuates above and below the ideal 2H<sub>2</sub>O and the average is close to the ideal value.

Various explanations can be suggested for the high values of Si, such as (1) the presence of colloidal silica which would not be seen in X-ray diffraction patterns, (2) a leaching of the analyzed materials which has removed some of the octahedral cations, (3) a contamination of the samples with a silica-rich impurity, such as a 2:1 layer silicate, e.g. talc. The third suggestion is unlikely because the amounts of impurity required to give the observed results would be considerable and they would probably be seen in the X-ray patterns, which in fact provide no evidence for such impurity levels. Suggestions (1) and (2) are essentially similar; if octahedral cations are removed from the edges of the layer structure, the residual silica will be equivalent to a rim of hydrated silica.

In the absence of any clear indication of the cause of the excess silica, we have re-calculated the formulae on the basis of three equivalent octahedral cat-

TABLE 1. Chemical Analyses and Formulae of Lizardites and Nepouites

	Lizardite		Nickel-Lizardite								Nepouite			
	(1)	(2)	(3)	(4)	(5)	(6)	(7)	(8)	(9)	(10)	(11)	(12)	(13)	(14)
SiO <sub>2</sub>	40.0	41.6	47.8	47.7	43.1	46.2	44.2	44.3	43.7	41.3	39.3	37.0	36.0	35.0
TiO <sub>2</sub>	0.03	0	0.03	0	0.02	---	---	---	---	0.01	0.01	0	0	---
Al <sub>2</sub> O <sub>3</sub>	1.60	0.83	0.38	0.24	0.26	0.54	0.25	0.52	0.24	0.18	1.02	0.21	0.18	0.47
Fe <sub>2</sub> O <sub>3</sub>	4.16	3.57	0.22	0.43	0.95	5.98	2.23	6.18	2.77	1.26	1.30	0.22	0.13	0.10
MgO	38.6	40.5	38.5	36.9	40.3	30.8	35.6	30.8	23.0	18.5	5.87	5.95	2.74	2.70
NiO	0.16	0.21	0.71	1.09	1.28	3.82	4.47	5.57	18.8	26.2	41.9	44.9	47.4	49.3
CaO	0.05	0.04	0.01	0.03	0	0.20	0.20	0.05	0.12	0.01	1.07	0.22	0.27	<0.05
Na <sub>2</sub> O	0.01	0	0.16	0.08	0.06	0.28	0.04	0.13	---	0.11	0.18	0.10	0.11	0.14
K <sub>2</sub> O	0.02	0.02	0.07	0.06	0.03	0.41	0.03	0.05	---	0.02	0.05	0.07	0.02	0.08
H <sub>2</sub> O <sup>+</sup> *	14.0	13.0	12.5	13.1	13.8	11.8	13.0	12.9	12.0	11.4	9.7	11.9	11.5	11.4
Total	98.6	99.8	100.4	99.6	99.8	100.0	100.0	100.5	100.7	99.0	100.4	100.6	98.4	99.2
(a) Formulae based on total cation valence = 14														
Si	1.93	1.95	2.16	2.19	2.02	2.16	2.09	2.11	2.18	2.17	2.19	2.16	2.19	2.13
Al <sup>IV</sup>	0.07	0.05												
Al <sup>VI</sup>	0.02	0.00	0.02	0.01	0.02	0.03	0.01	0.03	0.01	0.01	0.07	0.01	0.01	0.03
Fe <sup>3+</sup>	0.15	0.12	0.01	0.02	0.03	0.21	0.08	0.22	0.10	0.05	0.05	0.01	0.01	0.01
Mg	2.77	2.83	2.59	2.52	2.82	2.15	2.51	2.19	1.71	1.45	0.49	0.52	0.25	0.25
Ni	0.01	0.01	0.03	0.04	0.05	0.14	0.17	0.21	0.75	1.11	1.88	2.11	2.32	2.42
ΣOct **	3.03	3.02	2.67	2.61	2.95	2.65	2.81	2.77	2.63	2.65	2.55	2.66	2.60	2.73
Ca	0.00	0.00	0.00	0.00	0.00	0.01	0.01	0.00	0.01	0.00	0.06	0.01	0.02	0.00
Na	0.00	0.00	0.01	0.01	0.01	0.03	0.00	0.01	0.00	0.01	0.02	0.01	0.01	0.02
K	0.00	0.00	0.01	0.00	0.00	0.02	0.00	0.00	0.00	0.00	0.00	0.01	0.00	0.01
H <sub>2</sub> O <sup>+</sup>	2.25	2.04	1.89	2.01	2.15	1.84	2.05	2.05	2.00	2.00	1.79	2.31	2.33	2.32
(b) Formulae based on total equivalent octahedral cations = 3.00														
Si			2.00	2.00	2.00	2.00	2.00	2.00	2.00	2.00	2.00	2.00	2.00	2.00
Al			0.02	0.01	0.02	0.03	0.02	0.03	0.01	0.01	0.08	0.01	0.01	0.03
Fe <sup>3+</sup>			0.01	0.02	0.03	0.24	0.08	0.24	0.12	0.06	0.06	0.01	0.01	0.01
Mg			2.92	2.90	2.87	2.43	2.67	2.37	1.95	1.64	0.58	0.59	0.29	0.28
Ni			0.03	0.05	0.05	0.16	0.18	0.23	0.86	1.26	2.21	2.38	2.68	2.66
ΣOct			3.00	3.00	3.00	3.00	3.00	3.00	3.00	3.00	3.00	3.00	3.00	3.00
H <sub>2</sub> O <sup>+</sup>			2.00	2.00	2.00	2.00	2.00	2.00	2.00	2.00	2.00	2.00	2.00	2.00
Excess SiO <sub>2</sub>			0.43	0.52	0.06	0.45	0.23	0.29	0.49	0.46	0.58	0.44	0.53	0.34
Excess H <sub>2</sub> O <sup>+</sup>			0.12	0.31	0.19	0.08	0.19	0.22	0.28	0.27	0.11	0.61	0.69	0.55

\* H<sub>2</sub>O<sup>+</sup> = weight loss from 110° - 1100°C.

\*\* ΣOct = Σ(R<sup>2+</sup> + 3/2 R<sup>3+</sup>).

Analysts: #6, D. L. Bish; ##7,8,9,14, Pham Thi Hang; ##1,2,3,4,5,10,11,12,13, Hsien Ming Wan.

ions per formulae unit. The results are given under (b) in Table 1. The excess SiO<sub>2</sub> over the ideal 2SiO<sub>2</sub> and excess H<sub>2</sub>O<sup>+</sup> over 2H<sub>2</sub>O are listed separately. Although there is no basic reason for stating average values of the excess SiO<sub>2</sub> and H<sub>2</sub>O, since the samples come from different localities, the values in fact are: 0.40 SiO<sub>2</sub> and 0.30 H<sub>2</sub>O<sup>+</sup>, with a considerable range in each case.

**X-Ray Powder Diffraction Analysis**

Micro-crystalline chrysotiles and lizardites are difficult to characterize on the basis of X-ray powder diffraction patterns, but comparisons with patterns of well-established samples, including particularly lizardite from the type locality, leave little doubt that the nickel-containing minerals studied here closely resemble lizardite. This conclusion is supported by electron micrographs (Wan, 1975) which show poorly developed platy forms, generally crumpled, and often

forming fluffy aggregated masses; very few rod-like, fibrous, or tubular forms are seen.

Representative diffractometer patterns are shown in Figure 1, where (a) is the pattern of a lizardite from Kennack Cove, Lizard, England, the type locality, (b) and (c) are patterns of nickel lizardites, respectively samples 5 and 3 in Table 1, and (d) and (e) are patterns of nepouites, respectively 11 and 13 in Table 1. Patterns (a), (b), and (c) show marked enhancement of the basal reflections which is consistent with the platy morphology of the minerals; most of the nickel lizardites we have examined show this preferential orientation. The nepouites show less marked orientation, and their diffraction patterns generally are poorer than those of the lizardites.

A detailed discussion of the results can usefully begin with a consideration of the earlier work of Whittaker and Zussman (1956) on the characterization of serpentine minerals by X-ray diffraction, and

of Rucklidge and Zussman (1965) on the crystal structure of lizardite. The study of polytypism of trioctahedral 1:1 layer silicates by Bailey (1969) also is very relevant to the interpretation of the diffraction patterns. The poor resolution of most of the patterns is not conducive to a detailed study, but nevertheless some results can be obtained. From the earlier work on lizardites, it is evident that the basic 1:1 unit layers can be stacked in either an orthogonal or a monoclinic arrangement, there may be either one layer or two layers per unit cell, and various disordered combinations are possible. Rucklidge and Zussman remarked that X-ray powder patterns of lizardites "generally show no evidence of other than a single-layer cell with  $c \approx 7.3 \text{ \AA}$ , and  $\beta = 90^\circ$ ," but from single crystal data they found many disordered stackings. Therefore it is very interesting that, in the present work, we find nickel lizardites showing good evidence for a two-layer orthogonal structure. The best example is sample 5 from Valojoro, Madagascar. Attention is drawn particularly (Fig. 1, b) to the  $20l$  series of reflections with  $l$  taking both odd and even values. The indexed pattern is given in Table 2, where the calculated lattice spacings are based on  $a 5.298$ ,  $b 9.180$ ,  $c 14.605 \text{ \AA}$ . This mineral was studied previously

by Caillère (1936, p. 299, sample no. 112,857). A nickel lizardite from Morro do Niquel, Brazil (Table 1, sample 7) was previously recognized as having a two-layer, orthogonal structure (Brindley and Pham Thi Hang 1973, p. 29, Fig. 1c) but it is less well ordered than the Valojoro material.

In trioctahedral layer structures, the octahedral cations can occupy one of two sets of positions, which, following Bailey (1969), can be labelled I and II. An alternating sequence of type I and type II layers generates a two-layer unit, while type I or type II alone (they are equivalent) gives a single-layer cell. Mistakes in the layer type produce disordered structures and various degrees of disorder are possible. The two-layer orthogonal structure is the  $20r$  polytype of Bailey (1969) for which he calculated the powder diffraction intensities for a purely magnesian composition. These intensities, listed in Table 2, in many respects agree reasonably with the observed intensities. There are some anomalies, however, which may be related to structural disorders.

Most of the diffraction patterns recorded for nickel lizardites resemble pattern (c) in Figure 1. The  $20l$  diffractions are not seen for  $l$  odd and are scarcely seen for  $l$  even. In the region from  $34^\circ$ - $39^\circ$  ( $2\theta$ ), the

TABLE 2. X-ray Powder Diffraction Data for Nickel Lizardite, Valojoro, Madagascar (5, Table 1)

hk $l$	d (Å)				I			
	ortho	clino	obs.	calculated **		obs.	calc 2 Or	(Bailey, 1969) 2M <sub>1</sub>
				ortho	clino			
002			7.30	7.302		100	100	
020			4.55	4.590		30	23	
022			3.86	3.883		5	28	
004			3.65	3.651		90	68	
024			2.85	3.857		3	10	
200			2.65	2.650		5	6	
201			2.608	2.606		16	27	
	20 $\bar{2}$		2.547		2.534	3	--	12
202			2.493	2.490		50	51	
	202		2.442		2.441	15	--	100
				2.434			7	
006			2.329	2.327		15	78	
203			2.287	2.295		3	--	
040			2.143	2.144		10	18	
204			2.089		2.083	2	--	25
205			1.964	1.962		10	10	
008			1.827	1.826		3	1	
206			1.790	1.792		4	24	
310			1.734	1.725		5B	3	
028			1.687	1.696		4		
207			1.639	1.639		10		
060			1.530	1.530		35		
208			1.503	1.503		10		
00,10			1.459	1.460		3		
400			1.324	1.324		4		
402			1.307	1.303		10		

\*\*d (calc) from  $a 5.298$ ,  $b 9.180$ ,  $c 14.605$ ; for the monoclinic cell,  $d_{001} 14.605$ ,  $\beta = 93^\circ 20'$ .

strong 202 reflection broadens into a 'hump' with practically no clear characteristics. This degeneration of the diffraction pattern could be due to a mixture of monoclinic and orthogonal forms. Monoclinic structures are recognized by a separation of  $h0l$ ,  $h0\bar{l}$  pairs and  $hkl$ ,  $hk\bar{l}$  pairs; reflections with indices  $hk0$  and  $Ok\bar{l}$  are identical for the two systems. The pair of reflections most likely to be seen, if a monoclinic component is present, is the 202,  $20\bar{2}$  pair. For the  $2M_1$  polytype described by Bailey, the 202 reflection has the highest reflected intensity in the powder diagram; in Figure 1(b), it may be present weakly and  $20\bar{2}$  also may be visible. However, if a sample contains comparable amounts of the  $2M_1$  and  $2Or$  polytypes, the diffracted intensity from  $34^\circ$ - $39^\circ$  ( $2\theta$ ) may produce the unresolved 'hump' (Fig. 1c).

Nepouites generally give poorer X-ray diffraction patterns than lizardites. Typically (Fig. 1e) the basal reflections are broad and the 001 diffraction spreads towards smaller  $2\theta$  values; there may be an interstratification of layers with greater spacings. Most of this pattern consists of two-dimensional diffraction bands rather similar to those from other clay minerals. Evidently the stacking of the layers is highly disordered. Pattern (d) of Figure 1 shows a slight enhancement of the basal reflections and is the clearest nepouite pattern we have found so far. Besides the fourteen samples already described, many other samples were found which were mainly lizardites or nepouites, and which gave diffraction patterns similar to those already discussed. From the totality of this work, we draw the following conclusions:

(i) *Nepouites*: These are recognized by a 7.2-7.3 Å basal spacing and the general diffraction characteristics shown in Figure 1. The high nickel content is indicated by the intense, dark green color.

(ii) *Nickel lizardites*: These have a lighter green color and are considerably more common than nepouites. Like other lizardites, they give X-ray patterns indicating some three-dimensional order, and they appear to be commonly orthogonal rather than monoclinic. The diffraction patterns generally indicate considerable disorder, but at least two samples have been found with clear evidence for a two-layer orthogonal cell.

#### Thermal Behavior of Lizardites and Nepouites

Figure 2 summarizes the thermal behavior of lizardite (2), nickel lizardites (3, 4, 5, 10), and nepouites (11, 12, 13).

Each diagram shows the thermogravimetric

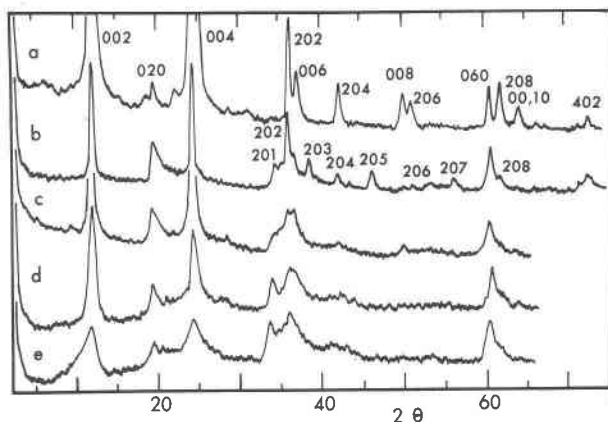


FIG. 1. X-ray diffractometer patterns of lizardites and nepouites.  $\text{CuK}\alpha$  radiation. (a) Lizardite, Kennack Cove, Lizard, England; (b) Nickel lizardite, #5 Valojoro, Madagascar; (c) Nickel lizardite, #3, Webster, North Carolina; (d) Nepouite, #11, Pavlos, Greece; (e) Nepouite, #13, New Caledonia.

(weight loss) curve and the phases formed at various temperatures under the heating conditions used. The amounts of the phases are represented schematically and are based on the intensities of the diffraction patterns. From these diagrams, the formation and decay of the transitional phases can be seen in relation to the dehydroxylation of the original minerals. Each diagram shows the weight loss,  $2\text{H}_2\text{O}$ , arising from the  $4(\text{OH})$  in the mineral formula. The excess  $\text{H}_2\text{O}+$  described earlier in relation to the chemical analysis (see Table 1, b) also is seen. It is important to recall that the samples used for X-ray examination and for the thermogravimetric curves were given identical heat-treatments, so that the two sets of data can be validly compared.

There are obvious differences between the thermal behavior of the low-nickel minerals (2, 3, 4, 5) and of the high-nickel minerals (10, 11, 12, 13). In all cases, dehydroxylation begins around  $450^\circ\text{C}$  and up to this temperature mainly the small amounts of excess  $\text{H}_2\text{O}+$  are lost. With low-nickel lizardites, dehydroxylation is about 80 percent complete by  $600$ - $650^\circ\text{C}$ . The remaining dehydroxylation takes place quite slowly and approaches completion near  $850^\circ\text{C}$ . With nepouites, dehydroxylation is clearly a two-stage process, with about three-quarters of the process complete at about  $700^\circ\text{C}$  and the remaining one-quarter at about  $1000^\circ\text{C}$ . The halt in dehydroxylation from about  $650^\circ$  to  $800^\circ\text{C}$  is very evident.

All the samples show the development of a long-spacing phase in the temperature range from about  $600^\circ$  to  $800^\circ\text{C}$ . This phase is marked LS in Figure 2 and is characterized principally by a broad diffraction

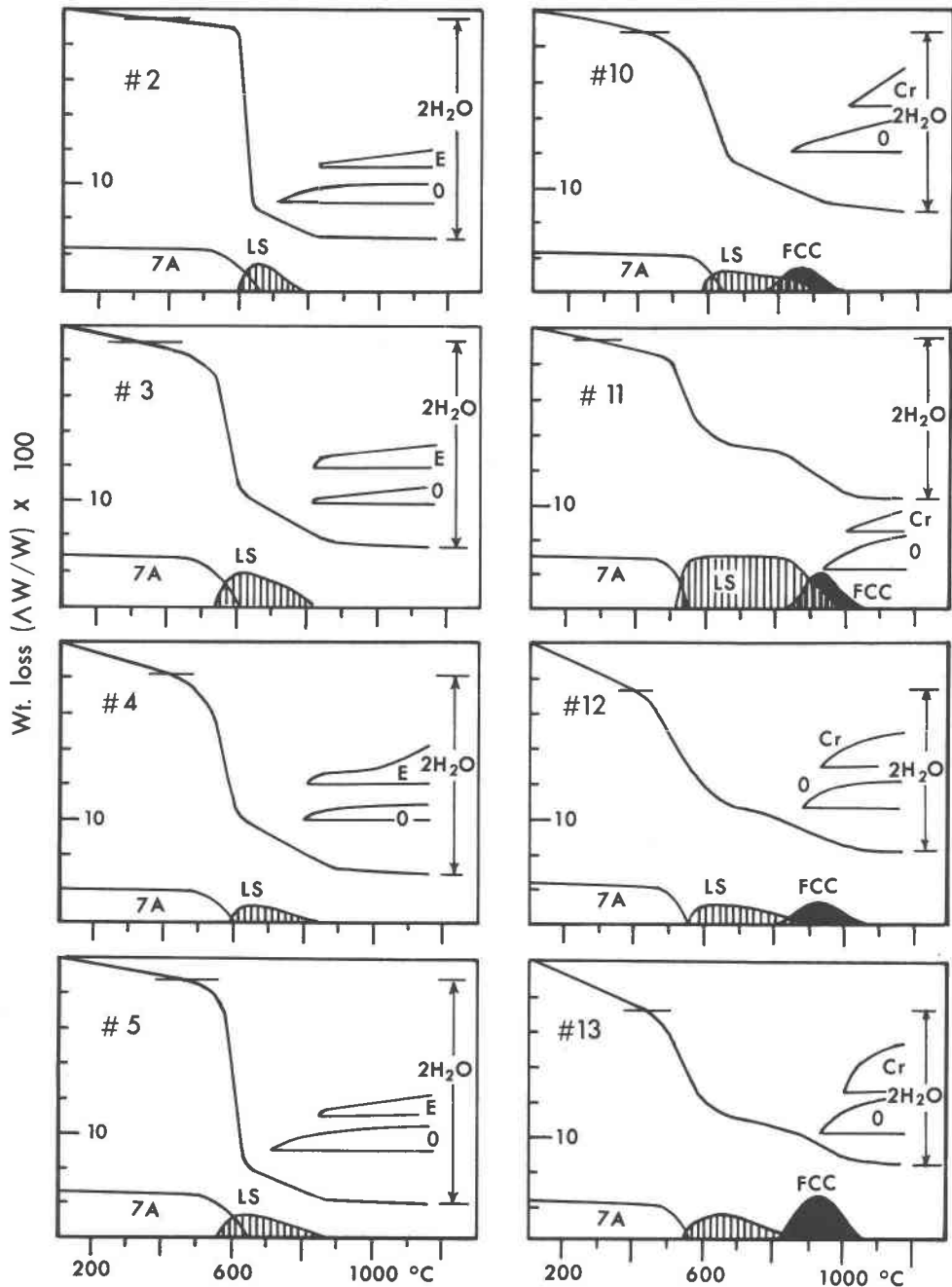


FIG. 2. Thermogravimetric curves and thermal transformations of lizardites and nepouites. Arrows show weight loss due to  $2\text{H}_2\text{O}$ , due to  $4(\text{OH})$  in the mineral formula. 7 Å-phase, initial mineral; LS, long-spacing phase; FCC, face-centered cubic phase; O, olivine; E, enstatite; Cr, cristobalite.

peak around  $6^\circ\text{-}8^\circ$  ( $2\theta$ ) corresponding to spacings around 14.5-11.5 Å. Typical diffraction patterns (Fig. 3) generally show the LS reflection to be very broad so that higher orders would not be expected, but sample 11 gives an exceptionally strong LS reflec-

tion and a third order, marked LS-3 in Figure 3, may be present.

The formation of the LS phase coincides with a rapid decay of the original basal reflections, but two-dimensional diffraction bands, including the

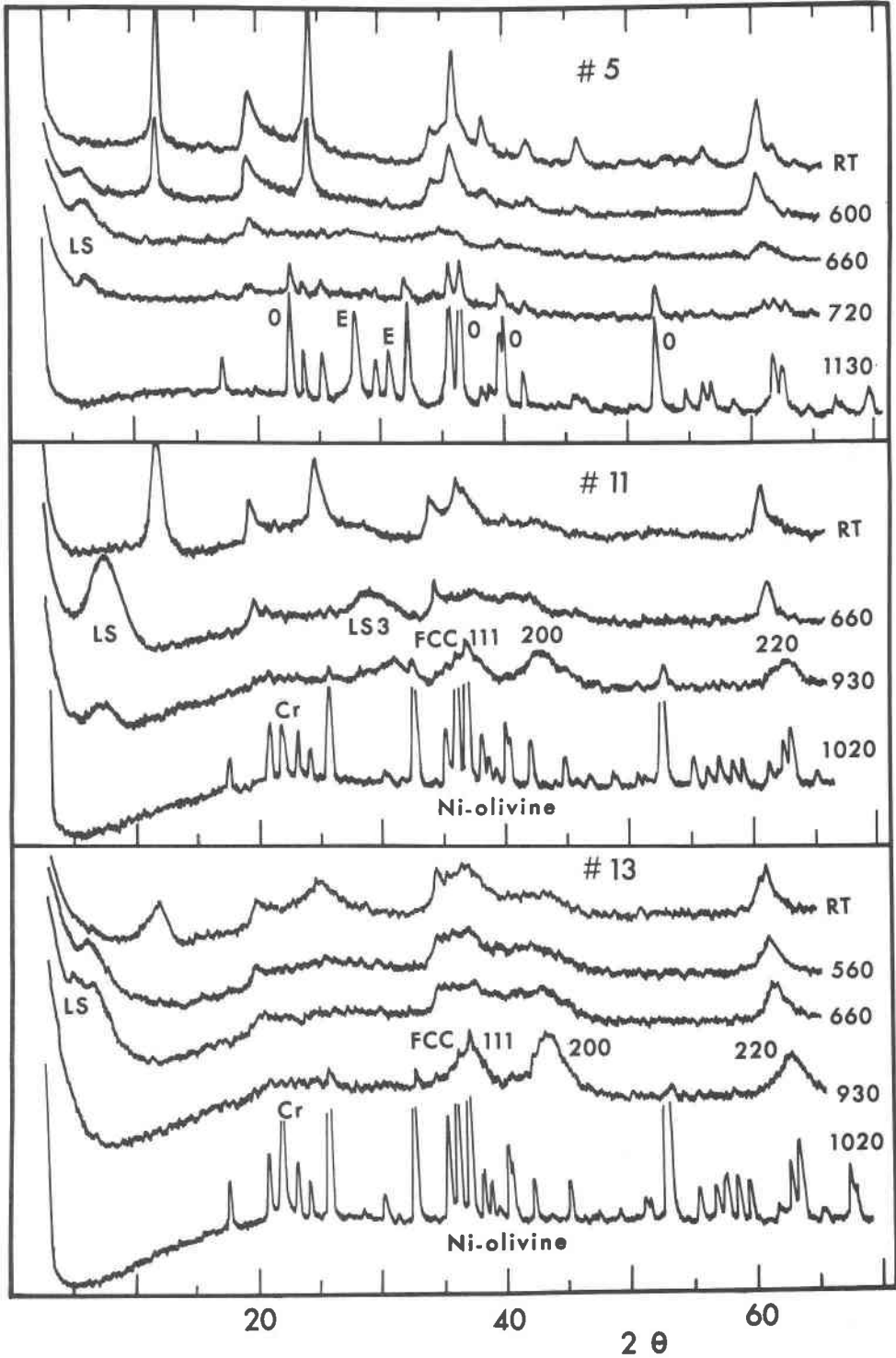


FIG. 3. Diffractometer patterns recorded after samples heated to stated temperatures. Samples: #5 from Valojoro, Madagascar; #11, from Pavlos, Greece; #13 from New Caledonia.

relatively sharp 06 band, persist. The 060 spacing shows a consistent change with temperature for all the samples studied. From room temperature to about 520°C there is essentially no change, but from 550° to about 800°C the 060 spacing gradually diminishes; a typical variation is from 1.528 to 1.505 Å. The other major characteristic of the LS phase is that it is formed in the temperature range where dehydroxylation is retarded. From these observations we conclude that the LS phase is a modified form of the original layer structure; it retains a significant proportion of structural 'water' (hydroxyl ions) and is formed by a reorganization of the layer structure normal to the layers, but it retains more or less the usual dimensions within the layers.

Nepouites develop a second transitional phase when the LS phase decays. This second phase is face-centered cubic and gives broad diffraction maxima (*cf* #11, #13 in Fig. 3) The cubic parameter cannot be precisely measured but the values obtained lie in the range  $a = 4.22 \pm 0.05$  Å, which may be compared with 4.178 Å for NiO and 4.213 Å for MgO, values taken respectively from ASTM cards 4-835 and 4-829. The jet black color is consistent with NiO. The color becomes bright green above 1000°C when the high temperature phases develop. The formation and decay of the face-centered cubic phase are evidently related to the second stage of dehydroxylation of nepouites.

The high-temperature phases, namely olivine and enstatite from low-nickel lizardites and olivine and cristobalite from high-nickel lizardite and nepouite, are in accordance with the MgO-NiO-SiO<sub>2</sub> equilibrium diagram as Pham Thi Hang and Brindley (1973) showed previously. The term 'olivine' is used in a general sense; Ni<sup>2+</sup> ions rather than Fe<sup>2+</sup> ions replace Mg<sup>2+</sup> ions of the forsterite structure. The spacings and intensities of the 'olivine' reflections vary with the proportion of Ni ions which are available.

### Discussion of the Transitional Phases

#### *The Long-Spacing Phase*

A transitional phase of this kind develops with all the serpentine minerals. A similar phase also is formed when dickite, among the kaolinite group minerals, is heated through the temperature range of dehydroxylation. With the data now available, some tentative suggestions can be made regarding the nature of the transformation. The fact that the spacing is usually in the range 13-14 Å suggests a chlorite-like arrangement. The retention of about one-quarter

of the hydroxyl 'water' of nepouites into the temperature range 600-800°C may correspond with the hydroxyl content of the 2:1 layer of a chlorite structure. (One quarter of the hydroxyls of the chlorite structure are located in the 2:1 layer). From these considerations it appears that the LS phase may resemble not so much the normal chlorite arrangement but rather a chlorite after the first stage of dehydroxylation.

Let us then review briefly the characteristics of chlorites after dehydroxylation of the interlayer hydroxide material. For magnesian chlorites, this stage of dehydroxylation occurs rather sharply around 500-550°C. The 001 reflection, from a 14 Å spacing, is greatly increased in intensity and the 001 ( $l = 2, 3, 4, 5$ ) reflections are considerably diminished. The spacing  $d_{001}$  may remain at 13.5-14 Å, but in the case of vermiculitized chlorites, it may decrease from 14 Å to values as low as 11 Å as the heating continues (Brindley and de Souza, 1975). Evidently, the diffraction characteristics of a chlorite after dehydroxylation of the interlayer material fit rather well with the corresponding observations for the LS phase developed in the present work.

The most reasonable interpretation we can suggest at present is the following: Nelson and Roy (1954) and Gillery and Hill (1959) showed that in hydrothermal experiments with appropriate gel compositions, chlorite structures were developed above about 450-500°C, but serpentine-type structures were formed at lower temperatures. When the process of crystallization at 600°C was followed progressively, serpentine structures were seen to form first and subsequently transform to the chlorite structure. The present experiments are far removed from hydrothermal conditions, but nevertheless hydroxyls are retained in an amount sufficient for the 2:1 layer of a chlorite-type structure. A layer structure persists as shown by the continued presence of the 060 reflection and the dimensions within the layer are little changed. It is not surprising that usually the only observed basal reflection from the LS phase is the first reflection, which is very strong from partially dehydroxylated chlorites. The persistence of the LS phase to around 800°C corresponds to the temperature range in which a chlorite persists prior to complete dehydroxylation and recrystallization.

#### *The Face-Centered Cubic Phase*

The black color and the lattice parameters are consistent with NiO, and the very broad diffraction maxima indicate very small nuclei. This phase develops

from the breakdown of the chloritic phase. Chlorites, however, do not show such a phase, nor do low-nickel lizardites. A high proportion of NiO in the mineral composition appears to be necessary. It is known that at the first stage of dehydroxylation of a chlorite, the decomposition of the interlayer hydroxide (the so-called 'brucitic' layer) gives a highly disordered form of MgO but observable nuclei of MgO have never been reported. Conceivably this may happen with NiO.

### Conclusions

Chemical, X-ray diffraction, and thermal data are given for 14 nickel-containing, serpentine-type minerals. Nickel lizardites, in which Ni ions occupy fewer than half the octahedral cation positions, tend to be better crystallized than nepouites, in which Ni ions occupy more than half the octahedral positions. The chemical analyses are consistent with a general formula  $R_3Si_2O_5(OH)_4$  together with a small, but variable amount of hydrous silica,  $x SiO_2$ ,  $y H_2O$ . The best crystalline material shows a two-layer, orthogonal structure which is close to the *2Or* polymorph of Bailey. The low-nickel containing minerals pass through a transitional phase showing a long-spacing in the range 14–11 Å between 600° and 800°C before recrystallizing to olivine and enstatite. The high-nickel containing minerals also pass through a long-spacing transitional phase from about 600° to 850°C or 900°C; from around 800 to 1000°C they show a face-centered cubic phase which may be a finely dispersed nickel oxide. The long-spacing phase retains appreciable 'water,' or hydroxyl ions, and may resemble a chlorite after the first stage of dehydroxylation. Recrystallization to olivine and cristobalite occurs at about 1000°C.

### Acknowledgments

This investigation forms part of a study of hydrous nickel silicates supported by grant GA 41413 from the National Science Foundation. We thank all individuals, companies, and organizations who have made materials available to us for this study. One of us (H.M.W.) thanks Mr. T. T. Feng, Director, Mining Research and Service Organization, Taipei, Taiwan, for leave of absence to participate in this work.

### References

- BAILEY, S. W. (1969) Polytypism of trioctahedral 1:1 layer silicates. *Clays Clay Minerals*, **17**, 355–371.
- BRINDLEY, G. W., AND PHAM THI HANG (1973) The nature of garnierites—I. Structures, chemical compositions, and color characteristics. *Clays Clay Minerals*, **21**, 17–40.
- , AND O. VON KNORRING (1954) New variety of antigorite (ortho-antigorite) from Unst, Shetland Islands. *Am. Mineral.* **39**, 794–804.
- , AND J. VIEIRA DE SOUZA (1975) Nickel-containing montmorillonites and chlorites from Brazil, with remarks on schuchardtite. *Mineral. Mag.* (in press).
- CAILLÈRE, S. (1936) Contribution à l'étude des minéraux des serpentines. *Bull. Soc. franc. Mineral.* **59**, 163–326.
- FAUST, G. T., J. J. FAHEY, B. MASON, AND E. J. DWORNIK (1969) Pecoraite,  $Ni_6Si_4O_{10}(OH)_8$ , the nickel analog of clinochrysotile, formed in the Wolf Creek meteorite. *Science*, **165**, 59–60.
- GILLERY, F. H., WITH V. G. HILL (1959) X-ray study of synthetic Mg-Al serpentines and chlorites. *Am. Mineral.* **44**, 143–152.
- GLASSER, E. (1907) Sur une espèce minérale nouvelle, la népouite, silicate hydraté de nickel et de magnésie. *Bull. Soc. franc. Mineral.* **30**, 17–28.
- JASMUND, K., AND H. M. SYLLA (1971a) Synthesis of Mg- and Ni-antigorite. *Contrib. Mineral. Petrol.* **34**, 84–86. (1971b) A correction. *Ibid.*, p. 346.
- MAKSIMOVIC, Z. (1973) Lizardite-nepouite isomorphic series. *Zapiski Mineral. Obsh.* **102**, 143–149.
- MEDLIN, J. H., N. H. SUHR, AND J. B. BODKIN (1969) Atomic absorption analysis of silicates employing  $LiBO_2$  fusion. *Atomic Absorpt. Newsl.* **8**, 25–29.
- NELSON, B. W., AND RUSTUM ROY (1954) New data on the composition and identification of chlorites. *Clays Clay Minerals*, **2**, 335–346.
- PHAM THI HANG AND G. W. BRINDLEY (1973) The nature of garnierites—III. Thermal transformations. *Clays Clay Minerals*, **21**, 51–57.
- RUCKLIDGE, J. C., AND J. ZUSSMAN (1965) The crystal structure of the serpentine mineral, lizardite,  $Mg_3Si_2O_8(OH)_4$ . *Acta Crystallogr.* **19**, 381–389.
- WAN, HSIEN-MING (1975) *The Lizardite-Nepouite and Kerolite-Pimelite Series of Minerals*. M.S. Thesis, The Pennsylvania State University.
- WHITTAKER, E. J. W., AND J. ZUSSMAN (1956) The characterization of serpentine minerals by X-ray diffraction. *Mineral. Mag.* **31**, 107–126.
- ZUSSMAN, J., AND G. W. BRINDLEY (1957) Serpentine with 6-layer orthohexagonal cells. *Am. Mineral.* **42**, 666–670.

*Manuscript received, March 3, 1975; accepted for publication, April 30, 1975.*